A Two Model Receptor System of the Alpha$_{1D}$ Adrenergic Receptor To Describe Interactions with Epinephrine and BMY7378

Debra L. Bautista,* Deanna H. Morris, Lauren Stein, Wesley Asher, and Timothy Hammitt

Chemistry Department, Eastern Kentucky University, Richmond, Kentucky 40475

Received April 9, 2005

In this study, we have developed a two receptor model system to describe the R and R* states of G-protein coupled receptors, specifically the alpha$_{1D}$ adrenergic receptor. The two models interact with agonist (epinephrine) and antagonist (BMY7378) differently. The active model has increased interactions with epinephrine. The inactive model has increased interactions with BMY7378. We also explored the protonation state of the ligands. When the most basic amine was protonated, we found increased hydrogen bonding and increased aromatic interactions. Protonated epinephrine hydrogen bonds with Asp176 and has aromatic residues Trp172, Trp235, Trp361, and Phe388 within 3 Å. Protonated BMY7378 hydrogen bonds with Trp172 and Lys236 and has aromatic residues Trp172, Trp254, Phe364, Phe384, and Phe388 within 3 Å. We conclude that the two model system is required to represent the two states of the receptor and that protonation of the ligand is also critical.

INTRODUCTION

G protein-coupled receptors (GPCRs) are characterized by seven transmembrane domains that span the lipid bilayer.[1] These domains are connected by intra- and extracellular loops. The GPCR super family includes rhodopsin, serotonin, dopamine, histamine, opioid, and adrenergic receptors.[2] These receptors mediate vastly diverse cellular responses including pain, vision, blood pressure, mood, and allergic reactions. Membrane receptors are extremely difficult to crystallize and to date only rhodopsin has been characterized crystallographically.[1] Therefore, other methods need to be used to identify key interactions between the receptor and the ligand.

The adrenergic receptors (ARs) are GPCRs that respond to biogenic amines including epinephrine and adrenaline.[3,4] ARs have nine members in three subclasses, the alpha 1, alpha 2, and beta.[5] These receptors mediate responses that include obesity, high blood pressure, and benign prostatic hyperplasia, which makes these receptors excellent targets for rational drug design.[2]

It is widely accepted that GPCRs have two states, R and R*. In the R state, the receptor is inactive and resting. This conformation of the receptor corresponds to our inactive model, and we propose that it will interact more efficiently with antagonists, specifically BMY7378. To activate the receptor, a conformation change takes place giving rise to the R* state. The R* state corresponds to the active model, and we propose that it will interact more efficiently with agonists, specifically epinephrine. One homology model will not depict both the R and R* states for this system.

Many groups have developed homology models of GPCRs including the ARs.[6−11] These models are based on ideal helices, bacteriorhodopsin, or on the crystal structure of bovine rhodopsin. After the structure of bovine rhodopsin was published,[1] using bacteriorhodopsin became clearly inadequate since bacteriorhodopsin is not a GPCR nor does it have high sequence homology to GPCRs.[12] Bissantz et al.[13] devised a virtual screening of three homology models using three docking programs and seven scoring functions. The receptor models were based on the crystal structure of bovine rhodopsin. This method was able to select antagonists from a database. It was not able to select any agonists. It is clear from this study that the crystal structure of bovine rhodopsin (PDB ID 1F88)[1] as a template creates models that represent the inactive state of the receptor. By combining this work with our own previous model of the EDG1 receptor,[11,14−18] we believe we can effectively model the interactions of both agonists and antagonists using this two model system.

To mimic the biochemical theory, our group has developed a two homology model system to identify the key interactions between alpha$_{1D}$ AR with both epinephrine (agonist) and BMY7378[19] (antagonist). Epinephrine and BMY7378, although structurally very different, have high affinity for the alpha$_{1D}$ receptor (K_i 35 and 8.6 nM, respectively). We propose that the active model, based on the previously published EDG1 ($S1P_1$) model, will interact more efficiently with an agonist. The inactive model (based on the crystal structure of bovine rhodopsin 1F88) will interact more efficiently with an antagonist. We also explored the effect of protonating the amine nitrogens of both epinephrine and BMY7378 to determine the effect of polar hydrogens on docking. The results of dynamics simulations of all docking complexes will also be presented.

METHODS

Homology Models. Two models of the alpha$_{1D}$ ARs were developed. Sequences from the National Center for Biotechnology Information (NCBI) were downloaded for the human

* Corresponding author phone: (859)622-1459; fax: (859)622-8791; e-mail: debra.bautista@eku.edu. Corresponding author address: 521 Lancaster Ave, Richmond, KY 40475.

10.1021/ci050116k CCC: $33.50
Published on Web 12/18/2005

Table 1. Sequences Used in Alignment of ARs[a]

chain	sequence	accession number
1	alpha$_{1A}$	NP_150646
2	rat alpha$_{1A}$	NP_058887
3	alpha$_{1B}$	NP_000670
4	hamster alpha$_{1B}$	P18841
5	alpha$_{1D}$	P25100
6	alpha$_{2A}$	NP_000672
7	alpha$_{2B}$	NP_000673
8	alpha$_{2C}$	P18825
9	beta$_1$	P08588
10	beta$_2$	P07550
11	beta$_3$	P13945
12	bovine rhodopsin	1F88[b]

[a] All sequences are human unless otherwise noted. [b] PDB ID.

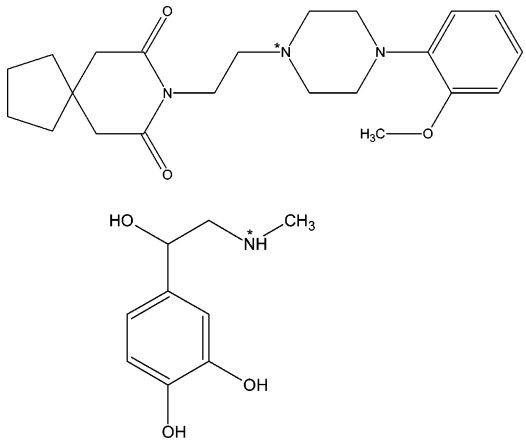

Figure 1. Ligands used in docking studies of the alpha$_{1D}$ receptor. Top is BMY7378. Bottom is epinephrine. * Indicates locations that a polar hydrogen was added to generate protonated forms of each ligand.

ARs. See Table 1 for sequence accession numbers. These sequences were aligned with the crystal structure for bovine rhodopsin (PDB ID 1F88)[20] and the previously published EDG1 model[15,16] using the default settings in Molecular Operating Environment (MOE Chemical Computing Group, Montreal, Canada).[21] The alignment was manually adjusted to remove any gaps from the seven transmembrane domains and to align the most conserved residue from each helix.[22] See the Supporting Information for alignment and homology table. The active model used the EDG1 model for a template. The model was minimized to a root-mean-squared gradient (RMSG) of 0.1 kcal/mol Å using the Amber94 force field.[23] A protein report was generated to determine if any angles or dihedrals exceeded biochemical norms (outliers). All outliers were in loop regions, which were not used in this study and thus ignored. The inactive model template was the crystal structure of bovine rhodopsin (1F88 from the Protein Databank).[20] The model was minimized to the same gradient and used the same force field. The protein report also indicated that the dihedral angle outliers were in loop regions and thus ignored. Both protein reports are available in the Supporting Information.

Ligands. The ligands were built in MOE and minimized to an RMSG of 0.01 using MMFF94 force field.[24] Two models were generated for both epinephrine and BMY7378. In one model the compounds were neutral, and in the second the most basic nitrogens were protonated. See Figure 1.

Docking. Docking used the algorithm MOE Dock. The default settings were used with the exception of Tabu search. A Tabu search will disallow a previous docking location for subsequent docking runs to ensure that the entire docking volume is probed. For each position, 700 iterations were generated to optimize the interactions at a location. A database of 25 complexes for each receptor with each ligand was generated. MMFF94 force filed was used. Since scoring functions can have 9.11 kJ/mol residual standard error,[25] evaluation was done by visual inspection. Interactive forces between the ligand and the receptor include hydrogen bonding, aromatic interactions, and hydrophobic interactions. Of these, hydrogen bonding is the strongest interaction followed by aromatic interactions and last, hydrophobic interactions. Therefore, the best complex was judged to be the complex with the greatest number of hydrogen bonds to side chain atoms, aromatic interactions and placement in the helical bundle. The best complexes were then minimized to an RMSG of 0.1 kcal/mol Å using MMFF94 force field. The best complex was selected from the minimized complexes based on the same criteria.

Dynamic Simulations. The best complex for each ligand and receptor was then subjected to two molecular dynamics simulations. Dynamics were performed on all eight complexes two times generating 16 molecular databases. This calculation used NVT parameters (holding constant moles, volume, and temperature). The first simulation was performed for 1 fs time step with 60 ps of heating prior to the 100 ps equilibrium (data collection) phase as in ref 18. The second dynamics simulation was performed under the same conditions, but the simulation was extended to 1000 ps (1 ns). The output databases contained 100 entries collected during the equilibrium phase. The simulation calculated potential energy (U in kcal/mol), temperature (T in kelvins), pressure (P in Kpa), total energy (E, kinetic and potential in kcal/mol), and enthalpy (H, E + PV in kcal/mol).

RESULTS AND DISCUSSION

In this study, we have generated two models of the alpha$_{1D}$ receptor. The active model is based on the previously published EDG1 model.[11,14−18] The inactive model is based on the crystal structure of bovine rhodopsin.[1] By using two models for this system we propose that the inactive model will have increased interactions with an antagonist and the active model will have increased interactions with an agonist. We further propose that protonation of basic amines in the ligand will increase interactions between the receptor model and ligand.

Active Alpha$_{1D}$ Model. The active model of the alpha$_{1D}$ receptor was based on the experimentally validated EDG1 model. This model was minimized using the Amber94 force field. The model was determined to be within acceptable biochemical parameters using the protein report function in MOE. The active model had five cis-amide bonds. These residues were located in intracellular loops 1 and 3 and in the carboxy terminus. See the Supporting Information for the protein report. The model had alpha helical domains containing 21 (helix4) to 30 (helix3) residues. See Table 2. It is well-known that prolines cause kinks in alpha helical domains since the amino acid is constrained.[26] The active model had two proline kinks in helix 7 that were not present

Table 2. Residues in the Helical Domains for the Active and Inactive Models of the $Alpha_{1D}$ Receptor

helix	active model	inactive model
1	A94 − I118	A94 − A122
2	F134 − M156	V136 − 159
3	G165 − V196	G165 − V198
4	K212 − L233	E210 − L233
5	E250 − V272	E251 − V274
6	A346 − L370	K344 − L373
7	F384 − R411	G382 − L417

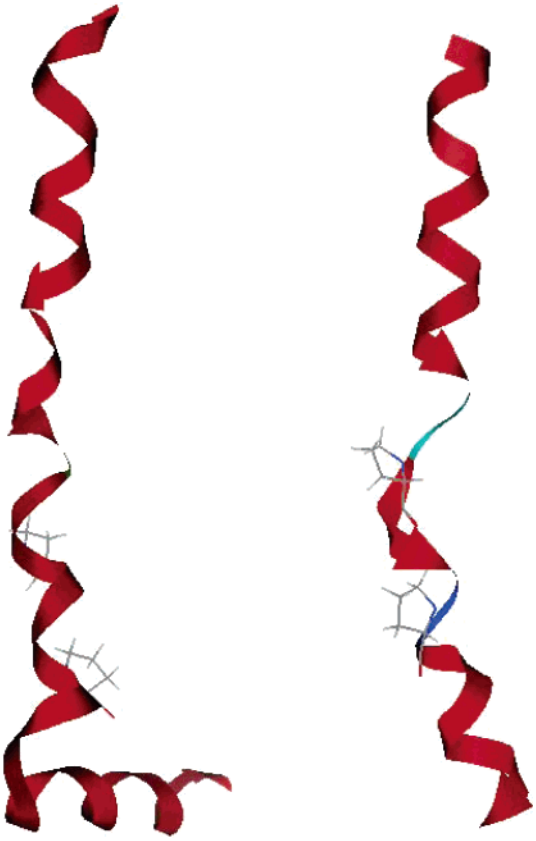

Figure 2. Helix 7 of the active (right) and inactive (left) models. Prolines in helix 7 are shown. The active model has two areas where loss of helical structure is shown. The inactive model has an alpha helical region that appears to be at the intracellular surface and is often called helix 8. This helix is not present in the active model due to the lack of crystal structure for that location.

in the inactive model even though both sequences have Pro399 and Pro403. See Figure 2.

$Alpha_{1D}$ Active with Epinephrine. Of the 25 docking runs, 4 had hydrogen bonds between the receptor and ligand. Only one entry had hydrogen bonds to side chains of the receptor. That complex was minimized to an RMS gradient of 0.1 kcal/mol Å. During that process hydrogen bonds to the side chain of Asp176 were lost, but hydrogen bonds were gained to the side chain of Cys396. Overall hydrogen bonding increased from 2 hydrogen bonds (Asp176 side chain and Asp142 backbone) to 5 (2 hydrogen bonds to the side chain of Cys396 and one each to Tyr392 and Phe388 both backbone interactions). The aromatic interactions both before and after minimization were to Phe388 and Tyr392. These interactions are only with helix 7. See Table 3 and Figure 3.

$Alpha_{1D}$ Active with Protonated Epinephrine. Of the 25 docking runs, 10 had hydrogen bonds between the ligand and receptor. Seven of those complexes were within the helical bundle. Many complexes were in overlapping or similar positions, and so only three complexes were selected for further minimization. Of the three minimized complexes, only one maintained and increased hydrogen bonding versus the initial structure. The best complex had two hydrogen bonds to the side chain of Asp176 before minimization. After minimization, the ligand had three hydrogen bonds to the side chain of Asp 176. The ligand was within 3 Å of aromatic residues Trp172, Trp235, Trp361, and Phe388 (helices 3, 6, and 7 and the loop between 4 and 5) after minimization. See Table 3 and Figure 4.

$Alpha_{1D}$ Active with BMY7378. Of the 25 docking runs only 3 had hydrogen bonds to the receptor. Two complexes were ruled out due to poor position and hydrogen bonds to backbone atoms. The best complex had one hydrogen bond to the side chain of Ser262 and aromatic interactions with Trp172, Trp235, Phe263, Trp361, Phe357, and Phe365. The helices involved were 3, 5, and 6 and the loop between helices 4 and 5. The interactions did not change during minimization. See Table 3 and Figure 5.

$Alpha_{1D}$ Active with BMY7378 Protonated. Of the 25 docking complexes only 4 had hydrogen bonds between the receptor and ligand. Three of the complexes had hydrogen bonds to side chain atoms of the receptor and were determined to be variations of the same position. One of these was selected for minimization. The minimized complex lost all hydrogen bonds. The ligand interacted with aromatic residues Trp172, Trp235, Tyr254, Trp361, and Phe384 both before and after minimization. The helices involved in aromatic interactions were 3, 5, and 6 and the loop between helices 4 and 5. See Table 3 and Figure 6.

We predicted that the active model would interact more efficiently with epinephrine than with BMY7378. We also predicted that the protonation state of the ligand would impact the docking results. With the active model, we had more hydrogen bonding between the receptor and the agonist

Table 3. Analysis of $Alpha_{1D}$ Active Model Docking with Epinephrine and BMY7378 Both Protonated and Neutral Forms[a]

ligand	K_i (nM)	hydrogen bonding residues	aromatic interaction residues	helices
		$Alpha_{1D}$ Active Model		
epinephrine protonated	35.1	3 to Asp176 sc	Trp172, Trp235, Trp361, Phe388	3, loop region 4−5, 6, 7
epinephrine		Gly391 bb, Phe388 bb, Tyr392 bb, 2 to Cys396 sc	Phe388, Tyr392	7
BMY7378 protonated	8.6		Trp172, Trp235, Tyr254, Trp361, Phe365, Phe384	5, loop region 4−5, 7, 3, 6
BMY7378		Ser262 sc	Trp172, Trp235, Phe263, Trp361, Phe365, Phe357	6, 5, 3, loop region 4−5

[a] bb indicates backbone hydrogen bond. sc indicates side chain hydrogen bond.

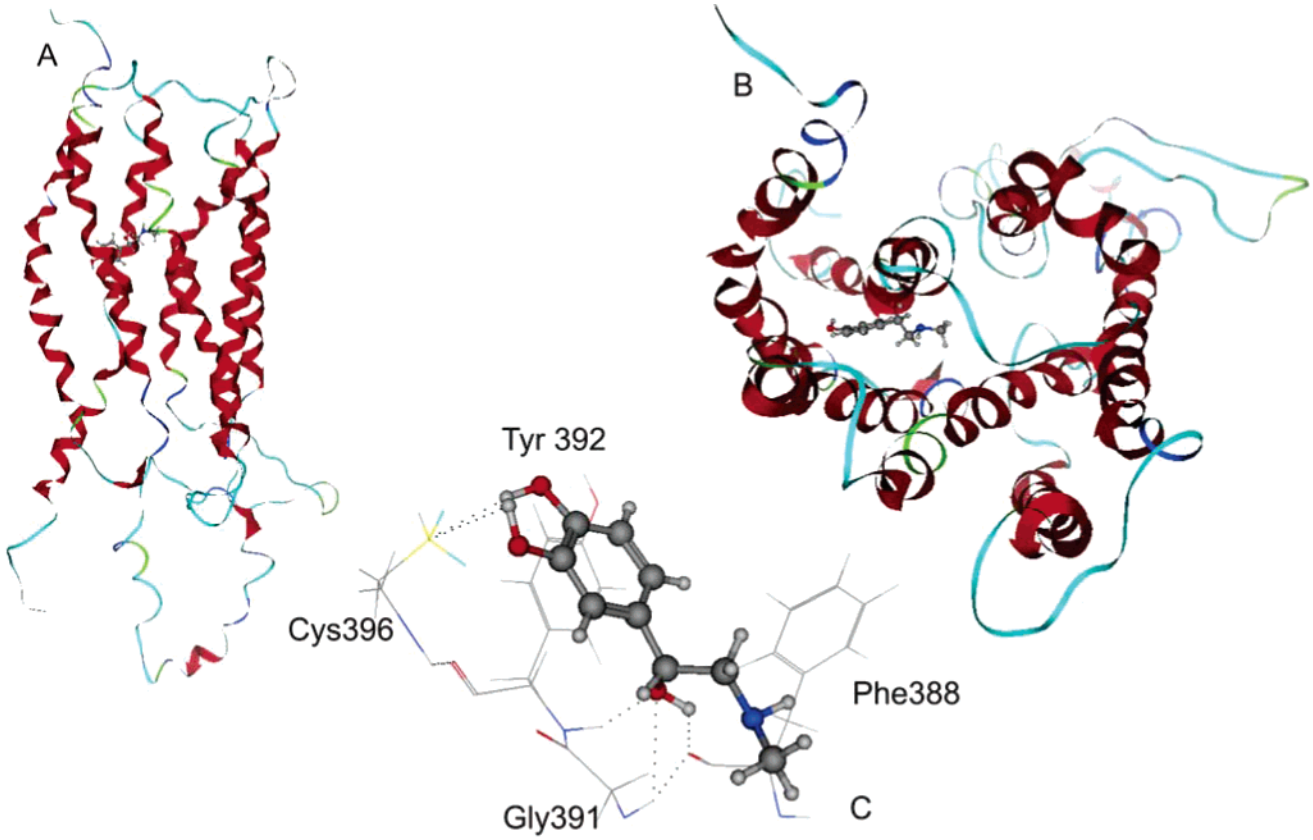

Figure 3. Epinephrine (neutral) with alpha$_{1D}$ active model. Panel A shows placement of the ligand in the receptor. Panel B is a view from the extracellular space into the helical bundle. Panel C highlights interactions of ligand and receptor.

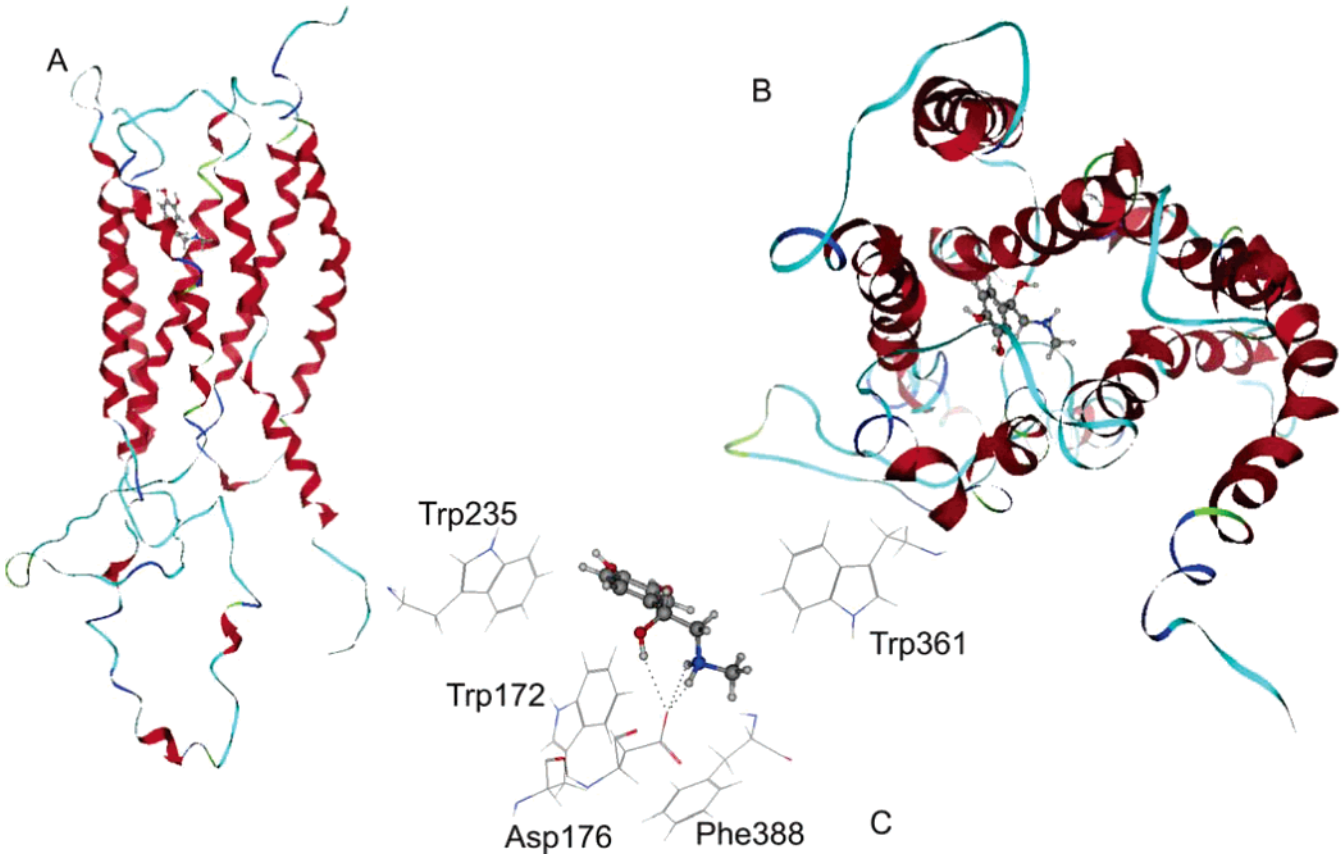

Figure 4. Epinephrine protonated with alpha$_{1D}$ active model. Panel A shows placement of ligand in the receptor. Panel B is a view from the extracellular space into the helical bundle. Panel C highlights interactions of ligand and receptor.

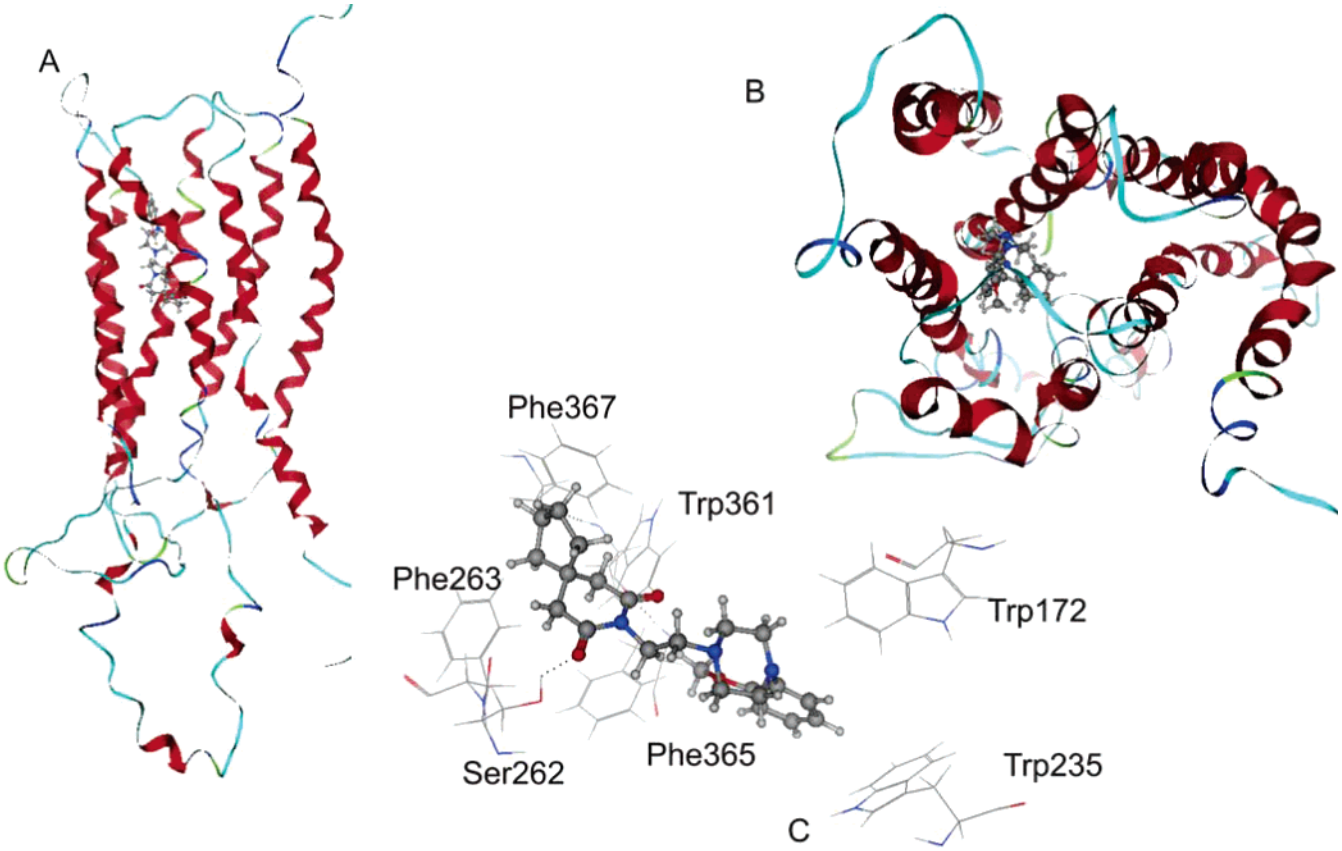

Figure 5. BMY7378 (neutral) with alpha$_{1D}$ active model. Panel A shows placement of the ligand in the receptor. Panel B is a view from the extracellular space into the helical bundle. Panel C highlights interactions of ligand and receptor.

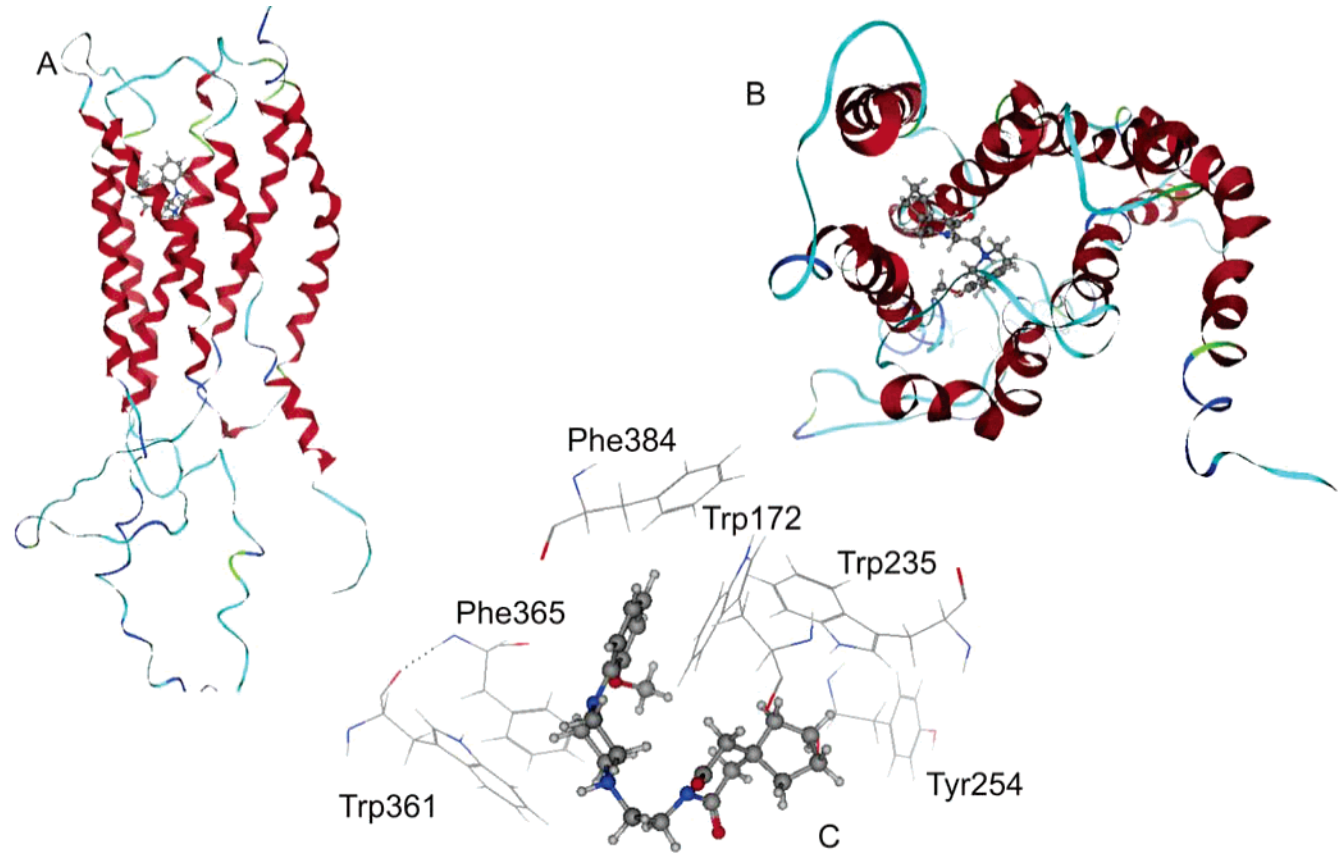

Figure 6. BMY7378 protonated with alpha$_{1D}$ active model. Panel A shows placement of the ligand in the receptor. Panel B is a view from the extracellular space into the helical bundle. Panel C highlights interactions of ligand and receptor.

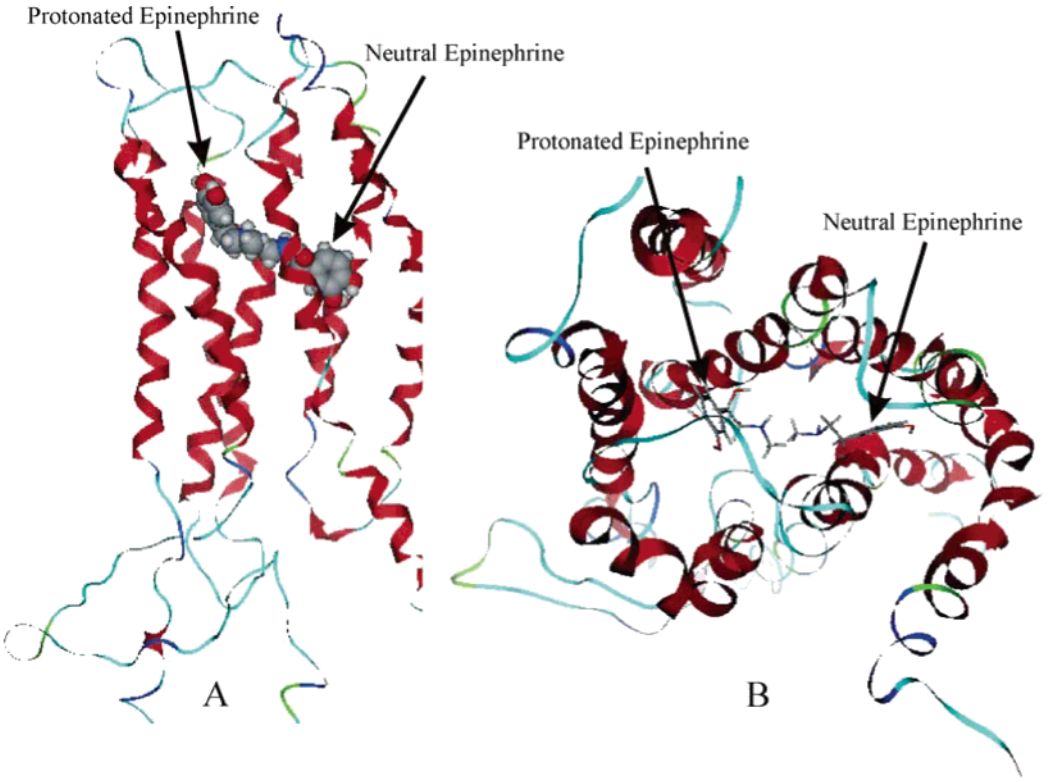

Figure 7. Placement of epinephrine in the active model. Panel A is a side view of the two molecules in the active model. Protonated epinephrine is located more toward the extracellular surface and to the left. Neutral epinephrine is to the right and more toward the center of the receptor. Panel B shows a view from extracellular space into the helical bundle. Protonated epinephrine is located on the left, and neutral epinephrine is on the right.

than with the antagonist. In both the agonist and the antagonist, we saw extensive interactions with aromatic residues. The protonation state of the ligand also had an effect on docking results. Hydrogen bonds to side chain atoms between active receptor and epinephrine were increased in the protonated form compared to the neutral form. The locations of the protonated and neutral forms of epinephrine are also interesting to note. The two are located in similar positions but tail to tail. See Figure 7. The placement of the protonated form is more central in the receptor, while the neutral form is lower. The large number of aromatic residues indicated some nonspecific interactions of the antagonist with the receptor.

Alpha$_{1D}$ Inactive Model. The inactive model of the alpha$_{1D}$ receptor used 1F88 as a template. The model was minimized using the Amber94 force field to a RMSG of 0.1 kcal/mol Å to prevent collapse of the binding site. The protein report indicated that there were nine cis dihedral angles outside of biochemical parameters. These dihedrals were in the highly variable third intracellular loop consisting of 70 residues located between helix 5 and 6. This loop was not indicated in any ligand receptor interactions, and therefore the cis-amide bonds were ignored. The transmembrane domains consisted of more than 20 residues for each helix. The two alpha$_{1D}$ models vary in the length and location of the helical domains but are generally very similar. The starting or ending residue for a helix is usually within 3 residues, with the exception of helix 7. In the inactive model, helix 7 starts 2 residues before the active model's helix and ends 6 residues later, giving rise to a helix of 35 residues for the inactive model and 27 residues for the active model. The early termination of the helix is due in part to the number of prolines in that helix. The differences in helix length between the two models may be due to deficiencies in the models or differences in the active versus inactive states of the receptor. However, it should be noted that a helix of 35 residues is unusually long and may extend into the intracellular space. Indeed, helix 7 of the inactive model is bent at the intracellular surface as shown in Figure 2. This intracellular helix is not present in the active model and may give some explanation for activation of the receptor, or it may be that the active model does not model intra- or extracellular loops effectively. See Table 3.

Alpha$_{1D}$ Inactive with Epinephrine. Of the 25 docking runs, 15 had hydrogen bonds between the receptor and ligand. Of the 15 complexes only 2 complexes were deemed appropriate for minimization due to hydrogen bonds to backbone atoms or placement in the helical bundle. In each case, the number of hydrogen bonds decreased to 1 (Ser153). In the two complexes, aromatic interactions were five and two residues each. Hydrogen bonding was clearly decreased from the active model, and the placement of the ligand in both models appeared to be partially but not completely overlapping. Aromatic residues are Phe102, Trp389, Phe388, Trp172, and Tyr392 from helices 1, 3, and 7. See Table 4 and Figure 8.

Alpha$_{1D}$ Inactive with Protonated Epinephrine. Of the 25 docking runs, 13 had hydrogen bonding between the receptor and ligand. Of the 13 only 3 were positioned within the helical bundle, and those were energy minimized. One entry completely lost all hydrogen bonds, while the second maintained only one hydrogen bond to backbone atoms. The last was determined to be the best complex since it had one hydrogen bond to the side chain of Tyr254. Aromatic

Table 4. Analysis of $Alpha_{1D}$ Inactive Model Docking with Epinephrine and BMY7378 Both Protonated and Neutral Forms[a]

ligand	K_i (nM)	hydrogen bonding residues	aromatic interaction residues	helices
		$Alpha_{1D}$ Inactive Model		
epinephrine protonated	35.1	Tyr254 sc	Tyr254, Trp361, Phe365	5, 6
epinephrine		Ser153 sc	Phe102, Trp172, Phe388, Trp389, Tyr392	1, 7, 3
BMY7378 protonated	8.6	Trp172 sc, Lys236 sc	Trp172, Tyr254, Phe364, Phe384, Phe388	3, 5, loop region 6−7
BMY7378		Thr181 sc, Tyr254 sc	Tyr254, Phe365	6, 5

[a] sc indicates side chain hydrogen bond.

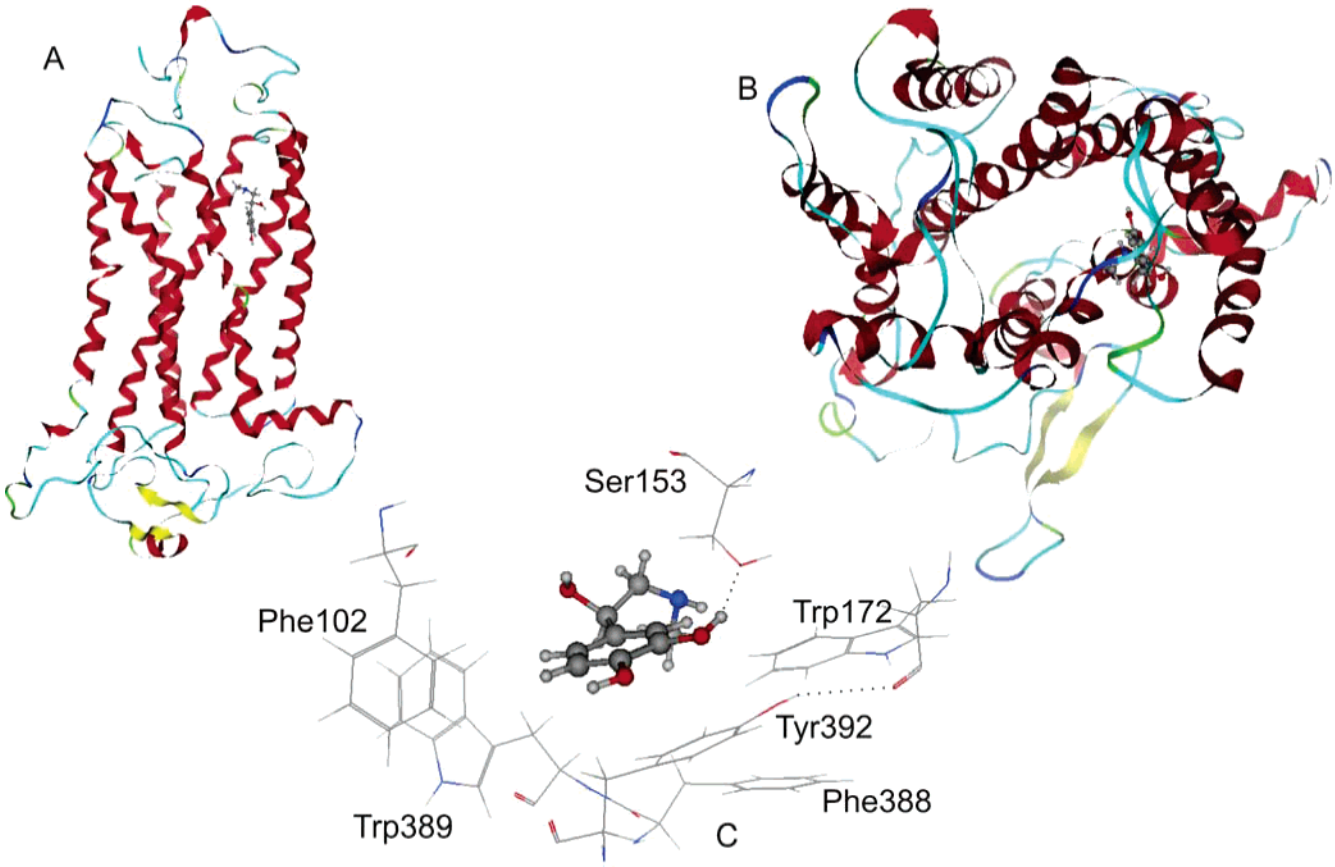

Figure 8. Epinephrine (neutral) with $alpha_{1D}$ inactive model. Panel A shows placement of the ligand in the receptor. Panel B is a view from the extracellular space into the helical bundle. Panel C highlights interactions of ligand and receptor.

interactions were similar for all three complexes: Tyr254, Phe365, and Trp361 from helices 5 and 6. See Table 4 and Figure 9.

$Alpha_{1D}$ Inactive with BMY7378. Of the 25 docking runs only 4 had hydrogen bonding with the receptor. Two of those were minimized based on position in the receptor and hydrogen bonding to side chain atoms. Both complexes had a hydrogen bond to Thr181 and one had hydrogen bonding to Tyr254. Aromatic interactions were limited to Tyr254 and Phe365 involving only helices 5 and 6. See Table 4 and Figure 10.

$Alpha_{1D}$ Inactive with BMY7378 Protonated. Of the 25 docking runs, only 5 had hydrogen bonds to the receptor. Three complexes were minimized based on position in the receptor and on hydrogen bonding to side chains. Two complexes decreased hydrogen bonding to one residue (Lys236 and Tyr392, respectively) during minimization. One had hydrogen bonding to two residues, Trp172 and Lys236 (see Table 4). This complex also had aromatic interactions with Tyr254, Phe384, Trp172, Phe388, and Phe364 located in helices 3 and 5 and the loop region between helix 6 and 7. This complex was determined to be the best. See Figure 11.

The inactive model clearly had more hydrogen bonds to the antagonist than to the agonist. In addition, the aromatic interactions increased in the protonated form over the neutral form. These interactions also involved helices 3 and 5 and the loop region between helices 6 and 7. Both the active and inactive models clearly had increased hydrogen bonding with the appropriate ligand. The protonation state of the ligand did not change hydrogen bonding but did impact aromatic interactions.

Dynamics. All complexes were subjected to molecular dynamics simulations twice. The output databases contained 100 entries collected during the equilibrium phase. Equilibrium phase for the two dynamic simulations was for 100 ps and 1000 ps. The simulation calculated potential energy, temperature, pressure, total energy (kinetic and potential), and enthalpy (E + PV). The average, standard deviation, and percent standard deviation were calculated for each dynamic run. Percent standard deviation was less than 3% for all variables over the entire simulation (data not shown).

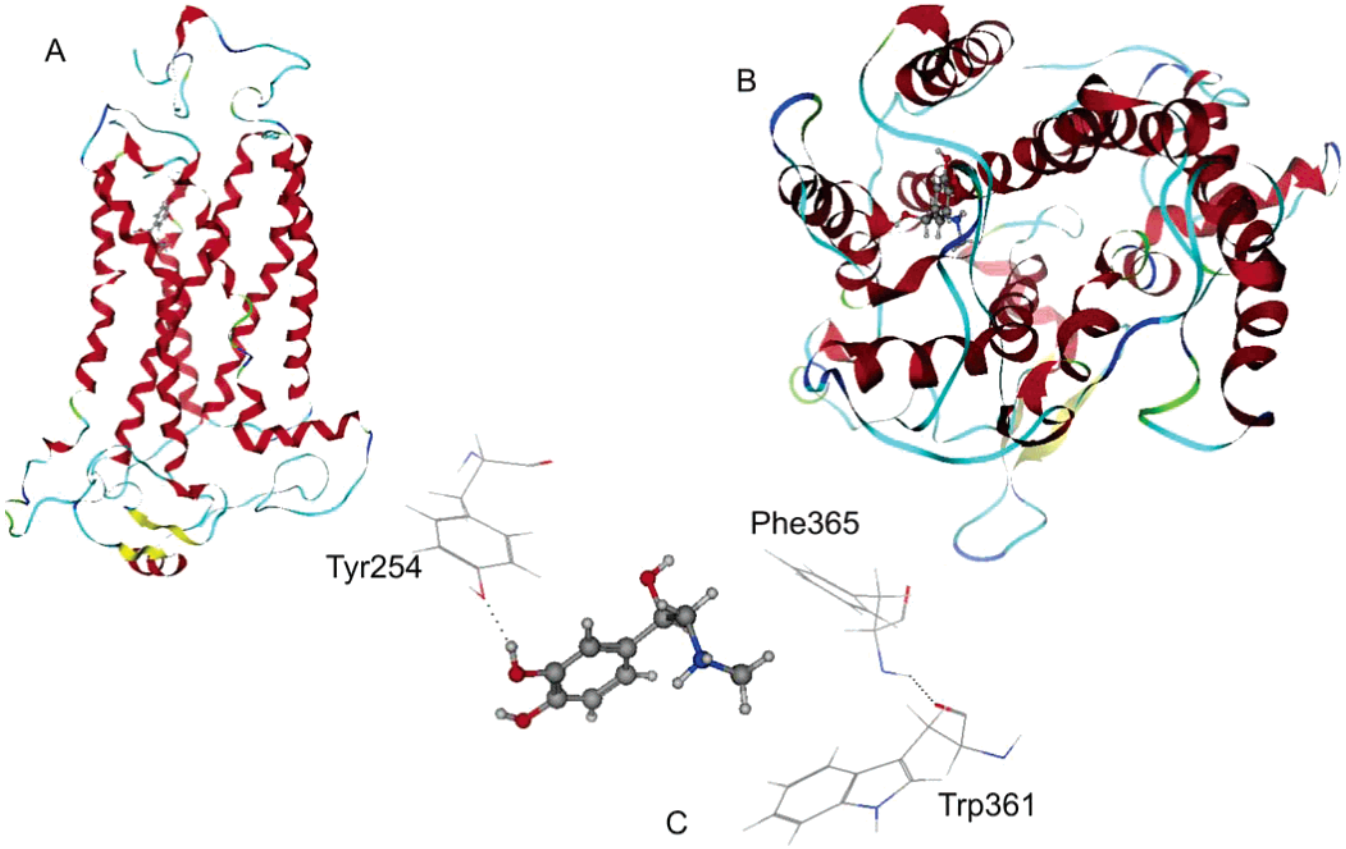

Figure 9. Epinephrine protonated with alpha$_{1D}$ inactive model. Panel A shows placement of the ligand in the receptor. Panel B is a view from the extracellular space into the helical bundle. Panel C highlights interactions of ligand and receptor.

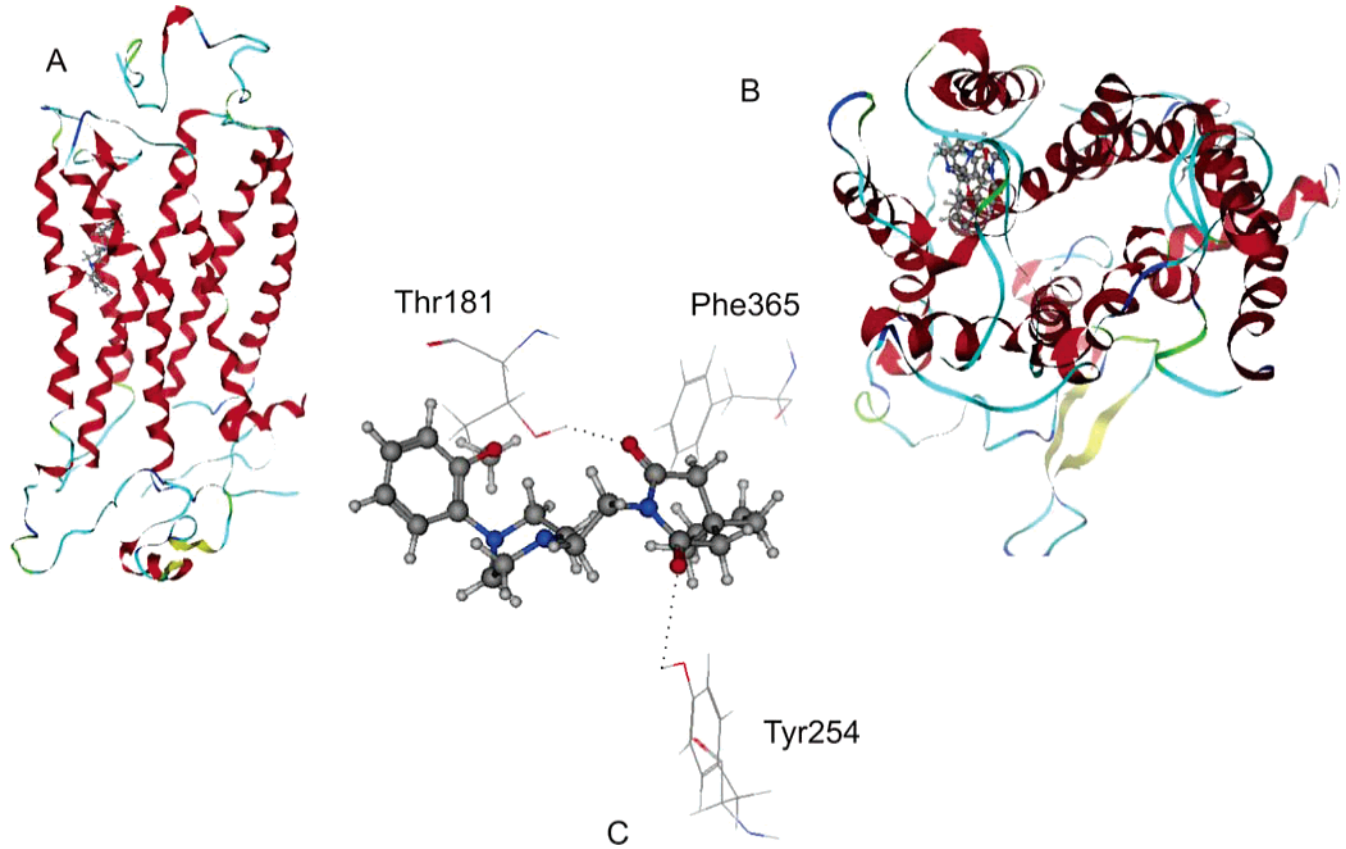

Figure 10. BMY7378 (neutral) with alpha$_{1D}$ inactive model. Panel A shows placement of the ligand in the receptor. Panel B is a view from the extracellular space into the helical bundle. Panel C highlights interactions of ligand and receptor.

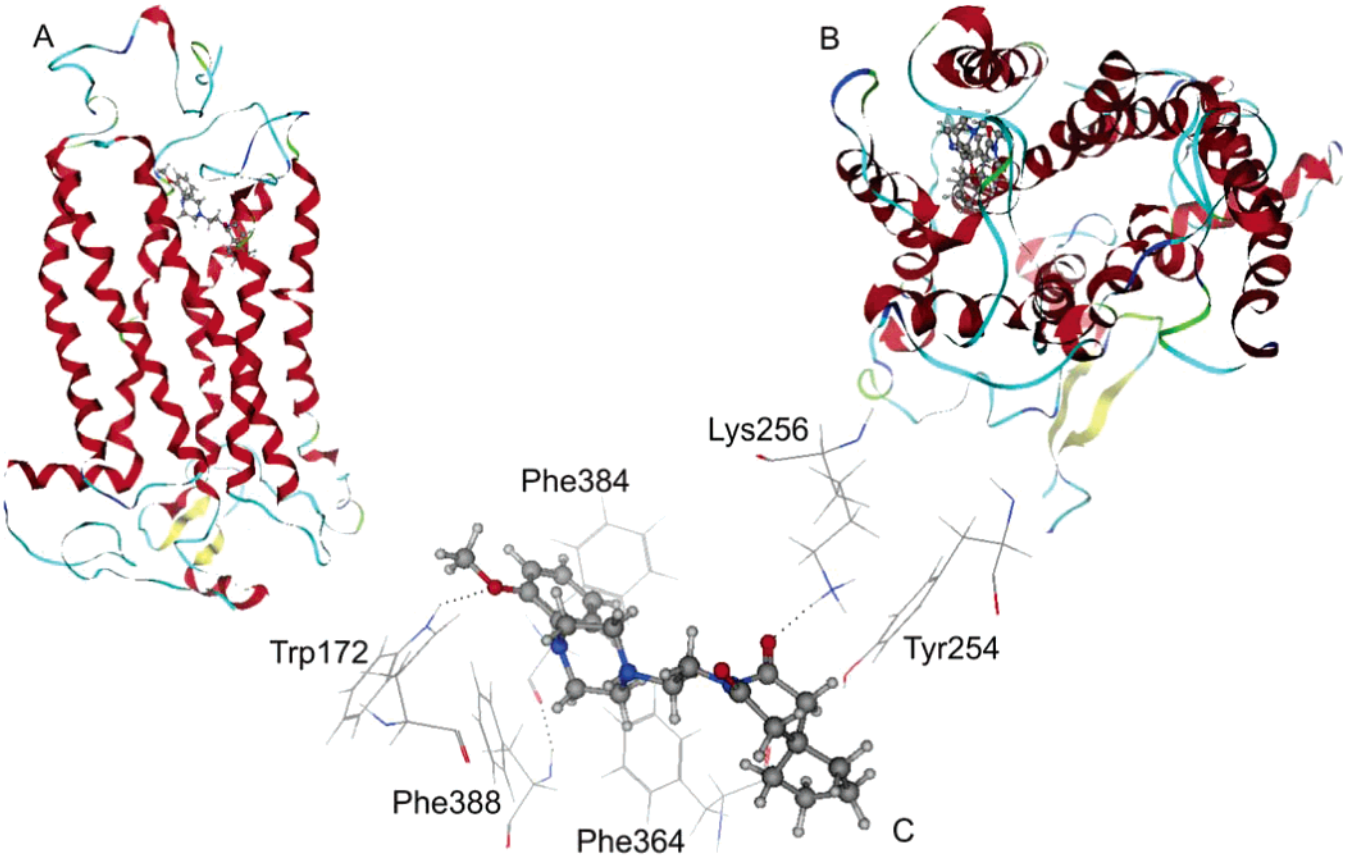

Figure 11. BMY7378 protonated with alpha$_{1D}$ inactive model. Panel A shows placement of the ligand in the receptor. Panel B is a view from the extracellular space into the helical bundle. Panel C highlights interactions of ligand and receptor.

All simulations were at equilibrium temperature and remained stable during the course of the calculations. The individual structures in the databases had momentary loss of alpha helical structure. However, the structure returned in subsequence entries. Therefore, the overall structure was stable for the simulation.

SAR Analysis. The mechanism of interaction between a receptor and ligand is a fundamental question of computational biochemistry. In the absence of a crystal structure of the protein and ligand, theoretical methods are frequently used to develop a hypothesis. The validity of a model can only be determined by crystallization. However, if a model correlates well with given experimental data or effectively predicts experimental data, the model can be used until more concrete data is available. Most information available concerning the AR family is in regard to the interactions between an agonist and the receptor. To determine the validity of the alpha$_{1D}$ AR model, we have compared the model to the experimental data available in the literature.

In 1987, Strader et al. determined that the aspartate (Asp113) of TMD III forms a salt bridge with the amine of the epinephrine.[27] This work used the hamster sequence of the beta$_2$ AR, which corresponds to D176 in the human alpha$_{1D}$ sequence. Our model of the active receptor and protonated epinephrine has two hydrogen bonds to Asp176. The carboxylate of aspartate forms hydrogen bonds to the benzyl hydroxyl and the amine of epinephrine.

Waugh et al. in 2001 determined that two phenylalanines were needed for antagonist binding.[28] This study, using the rat alpha$_{1A}$ AR, determined that mutation of either Phe308 (384) or Phe312 (388) greatly decreased affinity for some antagonists. No decrease of affinity was noted for phenylamine agonist binding (epinephrine type). Interestingly, imidazoline-type agonist affinity was effected by either mutation. This decrease in binding affinity would suggest two types of agonist binding. Our models of both the active and inactive receptors have either one or both of these residues within 3 Å of the ligand. The inactive model with BMY7378 has both residues within 3 Å, and the phenyl rings are oriented to allow for interaction of the rings. The active model with protonated epinephrine has only Phe388 within 3 Å. However, the phenyl ring of phenylalanine is not oriented so that the pi systems can overlap. The models are both in agreement with the experimental data to date. Future plans include docking of several inidazoline type agonists to determine if the phenylalanines interact with the ligand.

Greasley et al. reported that in the hamster alpha$_{1B}$ sequence a number of residues in helix 6 interact with residues in helix 3.[29] Mutation of Phe286 (340 in human alpha$_{1D}$), Ala292 (346), Leu296 (350), Val299 (353), Val300 (354), and Phe303 (357) increased inositol phosphate basal activity from 2- to 16-fold. The investigators concluded that the residues in helix 6 interacted with residues in helix 3 to stabilize the inactive form of the receptor and mutation of these residues created a constitutively active receptor. In our model of the inactive receptor, all but Phe286 (340) are within 3 Å of residues in helix 3. In the active model, only Val353 faces helix 3. The change in orientation of these residues in our two models correlates well with the experimental data.

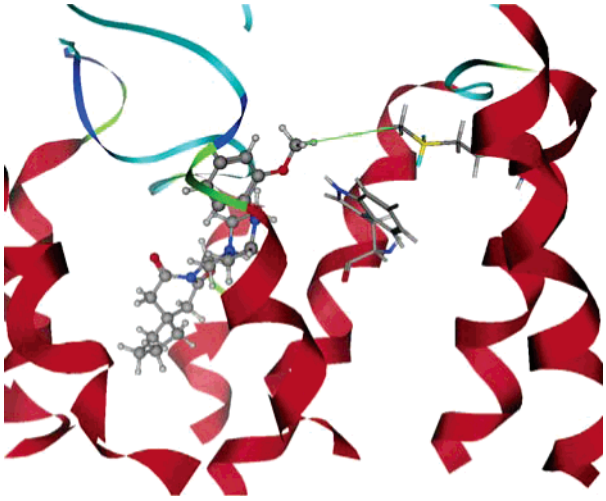

Figure 12. Close up of BMY7378 protonated in the inactive receptor model. Transmembrane domains are red alpha helices. Ligand is shown in ball-and-stick. Residues Met156 and W172 are shown in stick. Green line indicates the distance measured.

Two mutagenesis studies have identified that Ser200 (258) and Ser204 (262) in helix 5 are required for agonist binding.[27,30] These residues were identified in the alpha$_{2A}$ and beta$_2$ human ARs. There are currently no experimental data regarding these residues with respect to the alpha$_{1D}$ AR. In our models, Ser258 and Ser262 do not form hydrogen bond with the hydroxyl groups of the benzene ring. The serines are too far away to impact binding directly, but the loss of these two residues could impact the local structure. However, Ser259 is oriented toward the binding site and could impact binding although it is not hydrogen bonded to epinephrine. Ser258 and Ser262 are oriented toward helix 4 and may impact affinity due to helical packing or hydrogen bonding through water.

Hwa and workers mutated several residues of the hamster alpha$_{1B}$ AR into the corresponding residue in the rat alpha$_{1A}$ AR.[30,31] The mutations were predicted to change the binding profile of the alpha$_{1B}$ AR into that of the alpha$_{1A}$. Of the residues mutated, only Ala204 (alpha$_{1B}$ hamster) and Leu314 were determined to have any effect on binding affinity. The mutation of the alpha$_{1A}$ AR sequence with the residues of the alpha$_{1B}$ AR sequence reversed the binding profile. These residues are oriented toward the binding site of the receptor and can impact the binding profile in humans. Our alignment shows that this position may be important in subclass selectivity. In the alpha$_1$ ARs the residue is hydrophobic, in the alpha$_2$ ARs the residue is conserved as tyrosine and in the beta ARs it is conserved as asparagine.

Hamaguchi and workers published two of the few mutational studies involving alpha ARs regarding antagonists.[32,33] Presented in these studies is the first evidence that transmembrane domain 2 impacted binding. The mutation of alpha$_{1A}$ Phe86 to Met changed the binding profile from alpha$_{1A}$ to alpha$_{1D}$ for the four compounds tested. In the inactive model of the alpha$_{1D}$ in complex with BMY7378 protonated, we found that Met156 is 5.26 Å from the ligand. See Figure 12. This distance seems to be too far to directly impact the binding site. We propose that the increased bulk of phenylalanine at position 156 would cause a disruption of the hydrogen bond between Trp172 (in helix 3) and the ether oxygen in BMY7378. Future plans include testing of this hypothesis in the alpha$_{1A}$ receptor model currently under development.

Based on these papers, the active and inactive alpha$_{1D}$ models are in agreement with mutagenesis data and can be used to make predictions regarding residues needed for binding of epinephrine and BMY7378. Further studies are in progress to determine if the binding of other agonists and antagonists of the alpha$_{1D}$ AR differ significantly.

CONCLUSION

In this work, we have developed a two model system to describe the active and inactive states of the alpha$_{1D}$ AR. The docking studies indicated that the active model interacted more efficiently with epinephrine using hydrogen bonding, aromatic interactions, and position in the receptor model as the criteria for selecting the best complexes. The methylene hydroxyl and the amino groups of epinephrine specifically interacted with Asp176 which is supported by Strader et al.[27] Aromatic residues, including Phe388, are from helices 3, 6, and 7 and the extracellular loop between helices 4 and 5. Waugh et al. demonstrated the importance of Phe388 and Phe384.[28] The inactive model interacted more efficiently with the selective antagonist BMY7378. Protonated BMY7378 had hydrogen bonding with Trp172 and Lys236 of the inactive model. The antagonist also interacted with helices 3 and 5 and the loop region between helices 6 and 7. The aromatic residues indicated by this study for agonist and antagonist binding are similar but not completely overlapping. The complexes were subjected to two dynamics simulations, and all complexes maintained hydrogen bonding and aromatic interactions throughout the simulations. We are able to conclude from the dynamics simulation that the complexes are reasonable structures.[34] The protonation state of the ligand greatly impacted both hydrogen bonding as well as aromatic interactions. We also concluded that aromatic interactions were of great importance in the binding affinity of both agonists and antagonists.

ACKNOWLEDGMENT

Support was received from the NIH/NCRR/KBRIN, Grant # 1 P20 RR16841-01.

Supporting Information Available: The alignment, homology table, and protein reports for both models. This information is available free of charge via the Internet at http://www.pubs.acs.org.

REFERENCES AND NOTES

(1) Palczewski, K.; Kumasaka, T.; Horf, T.; Behnke, C. A.; Motoshima, H.; Fox, B. A.; Trong, I. L.; Teller, D. C.; Okada, T.; Stemkamp, R. E.; Yamamoto, M.; Muyano, M. Crystal Structure of Rhodopsin: A G Protein-Coupled Receptor. *Science* **2000**, *289*, 739−745.

(2) Klabunde, T.; Hessler, G. Drug design strategies for targeting G-protein-coupled receptors. *Chembiochem* **2002**, *3* (10), 928−44.

(3) Tranquilli, W. J.; Thurmon, J. C.; Benson, G. J. Alterations in the arrhythmogenic dose of epinephrine after adrenergic receptor blockade with prazosin, metoprolol, or yohimbine in halothane-xylazine-anesthetized dogs. *Am. J. Vet. Res.* **1986**, *47* (1), 114−8.

(4) Todd, E. P.; Vick, R. L. Kalemotropic effect of epinephrine: analysis with adrenergic agonists and antagonists. *Am. J. Physiol.* **1971**, *220* (6), 1964−9.

(5) Hancock, A. A.; Kyncl, J. J.; Martin, Y. C.; DeBernardis, J. F. Differentiation of alpha-adrenergic receptors using pharmacological evaluation and molecular modeling of selective adrenergic agents. *J. Recept. Res.* **1988**, *8* (1−4), 23−46.

(6) Chen, S.; Lin, F.; Xu, M.; Riek, R. P.; Novotny, J.; Graham, R. M. Mutation of a single TMVI residue, Phe(282), in the beta(2)-adrenergic receptor results in structurally distinct activated receptor conformations. *Biochemistry* **2002**, *41* (19), 6045−53.
(7) Fanelli, F.; Menziani, C.; Scheer, A.; Cotecchia, S.; De Benedetti, P. G. Ab initio modeling and molecular dynamics simulation of the alpha 1b-adrenergic receptor activation. *Methods* **1998**, *14* (3), 302−17.
(8) Mialet-Perez, J.; Green, S. A.; Miller, W. E.; Liggett, S. B. A primate-dominant third glycosylation site of the beta2-adrenergic receptor routes receptors to degradation during agonist regulation. *J. Biol. Chem.* **2004**, *279* (37), 38603−7.
(9) Wilcox, R. E.; Tseng, T.; Brusniak, M. Y.; Ginsburg, B.; Pearlman, R. S.; Teeter, M.; DuRand, C.; Starr, S.; Neve, K. A. CoMFA-based prediction of agonist affinities at recombinant D1 vs D2 dopamine receptors. *J. Med. Chem.* **1998**, *41* (22), 4385−99.
(10) Zuscik, M. J.; Porter, J. E.; Gaivin, R.; Perez, D. M. Identification of a conserved switch residue responsible for selective constitutive activation of the beta2-adrenergic receptor. *J. Biol. Chem.* **1998**, *273* (6), 3401−7.
(11) Parrill, A. L.; Wang, D.; Bautista, D. L.; Van Brocklyn, J. R.; Lorincz, Z.; Fischer, D. J.; Baker, D. L.; Liliom, K.; Spiegel, S.; Tigyi, G. Identification of Edg1 receptor residues that recognize sphingosine 1-phosphate. *J. Biol. Chem.* **2000**, *275* (50), 39379−84.
(12) Hoflack, J.; Trump-Kallmeyer, S.; Hibert, M. Re-evaluation of bacteriorhodopsin as a model of G protein-coupled receptors. *TiPS* **1994**, *15*, 7−9.
(13) Bissantz, C.; Bernard, P.; Hibert, M.; Rognan, D. Protein-based virtual screening of chemical databases. II. Are homology models of G-Protein Coupled Receptors suitable targets? *Proteins* **2003**, *50* (1), 5−25.
(14) Sardar, V. M.; Bautista, D. L.; Fischer, D. J.; Yokoyama, K.; Nusser, N.; Virag, T.; Wang, D. A.; Baker, D. L.; Tigyi, G.; Parrill, A. L. Molecular basis for lysophosphatidic acid receptor antagonist selectivity. *Biochim. Biophys. Acta* **2002**, *1582* (1−3), 309−17.
(15) Bautista, D. L.; Baker, D. L.; Wang, D.; Fischer, D. J.; Van Brocklyn, J.; Spiegel, S.; Tigyi, G.; Parrill, A. L. Dynamic Modeling of EDG1 Receptor Structural Changes Induced by Site-Directed Mutations. *THEOCHEM* **2000**, *529*, 219−224.
(16) Parrill, A. L.; Baker, D. L.; Wang, D.; Fischer, D. J.; van Brocklyn, J.; Spiegel, S.; Tigyi, G.; Bautista, D. L. Structural Features of EDG1 Receptor−Ligand Complexes Revealed by Computational Modeling and Mutagenesis. In *Lysophospholipids and Eicosanoids in Biology and Pathophysiology*; Goetzl, E. J., Lynch, K. R., Eds.; New York Academy of Sciences: New York, 2000; Vol. 905, pp 330−339.
(17) Fischer, D. J.; Nusser, N.; Virag, T.; Yokoyama, K.; Wang, D.; Baker, D. L.; Bautista, D.; Parrill, A. L.; Tigyi, G. Short-chain phosphatidates are subtype-selective antagonists of lysophosphatidic acid receptors. *Mol. Pharmacol.* **2001**, *60* (4), 776−84.
(18) Wang, D. A.; Lorincz, Z.; Bautista, D. L.; Liliom, K.; Tigyi, G.; Parrill, A. L. A single amino acid determines lysophospholipid specificity of the S1P1 (EDG1) and LPA1 (EDG2) phospholipid growth factor receptors. *J. Biol. Chem.* **2001**, *276* (52), 49213−20.
(19) Goetz, A. S.; King, H. K.; Ward, S. D.; True, T. A.; Rimele, T. J.; Saussy, D. L., Jr. BMY 7378 is a selective antagonist of the D subtype of alpha 1-adrenoceptors. *Eur. J. Pharmacol.* **1995**, *272* (2−3), R5−6.
(20) Berman, H. M.; Westbrook, J.; Feng, Z.; Gilliland, G.; Bhat, T. N.; Weissig, H.; Shindyalov, I. N.; Bourne, P. E. The Protein Data Bank. *Nucleic Acids Res.* **2000**, *28*, 235−242.
(21) *MOE*, 1998.10; Chemical Computing Group: Montreal, 1998.
(22) van Rhee, A. M.; Jacobson, K. A. Molecular Architecture of G Protein-Coupled Receptors. *Drug Dev. Res.* **1996**, *37*, 1−38.
(23) Cornell, W. D.; Cieplak, P.; Bayly, C. I.; Gould, I. R.; Merz, K. M. J.; Ferguson, D. M.; Spellmeyer, D. C.; Fox, T.; Caldwell, J. W.; Kollman, P. A. A Second Generation Force Field for the Simulation of Proteins, Nucleic Acids, and Organic Molecules. *J. Am. Chem. Soc.* **1995**, *117* (19), 5179−5197.
(24) Halgren, T. A. Merck Molecular Force Field. I. Basis Form, Scope Parameterization, and Preformance of MMFF94*. *J. Comput. Chem.* **1996**, *17* (5&6), 490−519.
(25) Morris, G. M.; Goodsell, D. S.; Halliday, R. S.; Huey, R.; Hart, W. E.; Belew, R. K.; Olson, A. J. Automated docking using a Lamarckian genetic algorithm and an empirical binding free energy function. *J. Comput. Chem.* **1998**, *19* (14), 1639−1662.
(26) Konvicka, K.; Ballesteros, J. A.; Weinstein, H. A Proposed Structure for Transmembrane Segment 7 of G Protein-Coupled Receptors Incorporating an Asn-Pro/Asp-Pro Motif. *Biophys. J.* **1998**, *75*, 601−611.
(27) Strader, C. D.; Sigal, I. S.; Register, R. B.; Candelore, M. R.; Rands, E.; Dixon, R. A. Identification of residues required for ligand binding to the beta-adrenergic receptor. *Proc. Natl. Acad. Sci. U.S.A.* **1987**, *84* (13), 4384−8.
(28) Waugh, D. J.; Gaivin, R. J.; Zuscik, M. J.; Gonzalez-Cabrera, P.; Ross, S. A.; Yun, J.; Perez, D. M. Phe-308 and Phe-312 in transmembrane domain 7 are major sites of alpha 1-adrenergic receptor antagonist binding. Imidazoline agonists bind like antagonists. *J. Biol. Chem.* **2001**, *276* (27), 25366−71.
(29) Greasley, P. J.; Fanelli, F.; Rossier, O.; Abuin, L.; Cotecchia, S. Mutagenesis and modelling of the alpha(1b)-adrenergic receptor highlight the role of the helix 3/helix 6 interface in receptor activation. *Mol. Pharmacol.* **2002**, *61* (5), 1025−32.
(30) Hwa, J.; Perez, D. M. The unique nature of the serine interactions for alpha 1-adrenergic receptor agonist binding and activation. *J. Biol. Chem.* **1996**, *271* (11), 6322−7.
(31) Hwa, J.; Graham, R. M.; Perez, D. M. Identification of critical determinants of alpha 1-adrenergic receptor subtype selective agonist binding. *J. Biol. Chem.* **1995**, *270* (39), 23189−95.
(32) Hamaguchi, N.; True, T. A.; Goetz, A. S.; Stouffer, M. J.; Lybrand, T. P.; Jeffs, P. W. Alpha 1-adrenergic receptor subtype determinants for 4-piperidyl oxazole antagonists. *Biochemistry* **1998**, *37* (16), 5730−7.
(33) Hamaguchi, N.; True, T. A.; Saussy, D. L., Jr.; Jeffs, P. W. Phenylalanine in the second membrane-spanning domain of alpha 1A-adrenergic receptor determines subtype selectivity of dihydropyridine antagonists. *Biochemistry* **1996**, *35* (45), 14312−7.
(34) Bautista, D. L.; Penn, W.; Simonetti, K. Computational Investigations of the Octameric Enolase Enzyme. *J. Ky. Acad. Sci.* **2005**, *66* (1).

CI050116K